2011

# ANN-Based Adaptive PI Control for Wind Turbine with Doubly Fed Induction Generator

Baohua Dong
*University of Nebraska–Lincoln*

Sohrab Asgarpoor
*University of Nebraska–Lincoln*, sasgarpoor1@unl.edu

Wei Qiao
*University of Nebraska–Lincoln*, wqiao@engr.unl.edu

North American Power Symposium (NAPS), 2011
doi: 10.1109/NAPS.2011.6025106

# ANN-Based Adaptive PI Control for Wind Turbine with Doubly Fed Induction Generator

Baohua Dong, Sohrab Asgarpoor, and Wei Qiao
Department of Electrical Engineering
University of Nebraska–Lincoln
Lincoln, Nebraska 68588-0511, USA
sasgarpoor1@unl.edu; wqiao@engr.unl.edu

*Abstract*—**This paper focuses on developing a novel algorithm which dynamically optimizes the controllers of doubly fed induction generator (DFIG) driven by a wind turbine (WT) to increase DFIG transient performance in all wind speed conditions. Particle swarm optimization (PSO) is proposed to optimize parameters of PI controllers of DFIG's rotor side/grid side converters (RSC/GSC) at different wind speeds in order to maximize the damping ratios of the system eigenvalues in small signal stability analysis. Based on the optimal values and the wind speed data set, an artificial neural network (ANN) is designed, trained, and it has the ability to quickly forecast the optimal values of parameters. Adaptive PI controllers (including ANN) are designed which dynamically change PI gain values according to different wind speeds. Simulation is done via PSCAD software for a single machine connected to an infinite bus (SMIB) system. The results show that the DFIG of ANN-based adaptive PI control could significantly contribute in the transient performance improvement in a wide wind speed range.**

*Index Terms*—**Particle swarm optimization, DFIG, small signal stability, artificial neural network, damping ratio, optimal control, transient performance, and PSCAD**

## I. Introduction

Wind power capacity is growing at the rate of 20% annually on the average in the world, and its cost has decreased 50% in the last 10 years [1]. The quickly increasing widespread use of wind power extensively reduces carbon emissions, reduces the effect on global warming, and cuts down the dependence on fossil fuels.

With the rapid developments in power electronics, DFIG-WTs are very popular and the worldwide market share of DFIG is approximately 30% in recent years because of the advantages of higher efficiency, operation in a wide range, reactive power production, lower cost, and flexible control [2-6].

With the increasing high penetration of wind power, DFIG plays a more important role in power systems stability, and the improvement of DFIG transient performance is becoming increasingly significant. Previous researchers have attempted to improve this by developing different algorithms in the past 10 years. In [7], the authors investigated and compared the different crow bar protections and rotor side converter restart schemes to improve DFIG transient performance. A new series and parallel connected grid side converters with conventional DFIG was developed to damp out the stator and rotor currents oscillations in [8]. In another paper [9], the authors proved that adding a power system stabilizer to large wind farms could significantly influence network damping and achieved a good voltage control capacity. In [10], the authors presented an energy capacitor system with a fuzzy-logic-controlled reference signal adjuster in the converter control to smoothen the output fluctuation. Others developed a PSO algorithm to design the optimal PI controllers for the rotor-side converter to improve the transient performance [11]. The authors in [12] developed PSO to design the optimal PI controllers for the rotor side converter and grid side converter of DFIG for a particular wind speed. More recently, the authors in [13] presented Bacteria Foraging technique to separately optimize the parameters of DFIG and the damping controller to increase the damping of low frequency angular oscillations of DFIG in three different wind speeds.

However, all of the approaches so far only optimize the controller parameters at one special operating point (fix-optimal model) and the parameters are constant. The controllers don't have the ability to dynamically adjust the PI gain values according to the wind speed difference. Secondly, these approaches are based on SMIB system and the impacts of transmission lines and multi-machines are simply neglected.

The proposed ANN-based adaptive PI control DFIG model is designed to improve DFIG transient performance. PSO is used to optimize PI parameters of DFIG's rotor and grid side converters at different operating points (different wind speeds) in order to maximize the damping ratios of the system eigenvalues in small signal stability analysis. Based on the calculated optimal values and the given wind speed data set, a two-layer feed-forward artificial neural network is designed and trained. The calculation for optimization and training is relatively slow and is done off-line. After that, ANN has the ability to quickly forecast the optimal values at each wind speeds. The calculation for prediction is relatively fast and is done on-line. A sensor captures the wind speed which is ANN's input, and ANN forecasts the optimal values and outputs them into the smart PI controllers. The controllers dynamically change values according to the different wind speeds to increase DFIG transient performance in a global operating range.

The contributions of this paper are as follows:

*1)* **Adaptive controllers**: In the new algorithm, ANN controllers smartly adjust the PI parameters to the optimal state and improve the transient performance of DFIG in a wide wind speed range.

*2)* **Real-time optimization**: This paper realizes real-time optimization by training ANN to forecast the optimal values and transferring much calculation to be done off-line. ANN controllers are optimized in real-time according to the different operating points.

*3)* **Fast and accurate prediction**: ANN controllers can predict the optimal values fast and accurately because the suitable and efficient structure is selected in the novel algorithm.

This paper is structured as follows. Section II mainly presents DFIG-WT models. Section III introduces small signal stability analysis. Section IV states PSO optimization and ANN training. Section V analyzes the simulation and results. Section VI gets the conclusions.

## II. DFIG-WT MODELS

The single machine (DFIG) connected to an infinite bus system (SMIB) is shown in Fig. 1. The components considered include wind turbine, induction generator, the back-to-back converter system, transmission line and the grid. These components are well established in [11]. They are briefly introduced in the following sections for the sake of completeness of the paper.

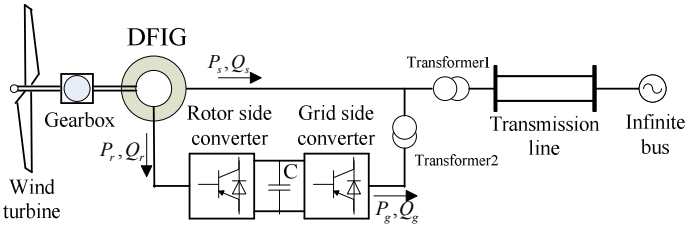


Fig. 1. DFIG-WT SMIB system.

### A. Induction Generator Model

The induction generator in this paper is a single-cage wound rotor induction machine and applied synchronously rotating reference frame transformation [14] to derive the voltage, flux linkages and transient voltage equations [15]:

$$v_{ds} = r_s i_{ds} - \omega_s \lambda_{qs} + p\lambda_{ds} \tag{1}$$

$$v_{qs} = r_s i_{qs} + \omega_s \lambda_{ds} + p\lambda_{qs} \tag{2}$$

$$v_{dr} = r_r i_{dr} - (\omega_s - \omega_r)\lambda_{qr} + p\lambda_{dr} \tag{3}$$

$$v_{qr} = r_r i_{qr} + (\omega_s - \omega_r)\lambda_{dr} + p\lambda_{qr} \tag{4}$$

$$\lambda_{ds} = L_s i_{ds} + L_m i_{dr} \tag{5}$$

$$\lambda_{qs} = L_s i_{qs} + L_m i_{qr} \tag{6}$$

$$\lambda_{dr} = L_m i_{ds} + L_r i_{dr} \tag{7}$$

$$\lambda_{qr} = L_m i_{qs} + L_r i_{qr} \tag{8}$$

$$e'_{ds} = -\omega_s \lambda_{qr} L_m / L_r \tag{9}$$

$$e'_{qs} = \omega_s \lambda_{dr} L_m / L_r \tag{10}$$

where $v_{ds}, v_{qs}, v_{dr}, v_{qr}, i_{ds}, i_{qs}, i_{dr}, i_{qr}, \lambda_{ds}, \lambda_{qs}, \lambda_{dr}, \lambda_{qr}, \omega_s, \omega_r, e'_{ds}, e'_{qs}, r_s, r_r$ are the d/q axis stator/rotor voltages/currents/flux linkages, the synchronous reference speed, the generator rotor speed, the d/q axis stator transient voltages, and the stator/rotor resistors, respectively. Also, $L_s = L_{ls} + L_m, L_r = L_{lr} + L_m, ; L_{ls}, L_{lr}, L_m$ are the stator leakage inductance, the rotor leakage inductance, and the mutual inductance, respectively. Substituting (9) and (10) into (7) and (8), we get:

$$i_{dr} = \frac{e'_{qs}}{L_m \omega_s} - \frac{L_m i_{ds}}{L_r} \tag{11}, \qquad i_{qr} = \frac{-e'_{ds}}{L_m \omega_s} - \frac{L_m i_{qs}}{L_r} \tag{12}$$

The flux linkage variables are now eliminated by substituting (9), (10), (11), and (12) into (3) and (4), as:

$$pe'_{ds} = s\omega_s e'_{qs} - \frac{r_r e'_{ds}}{L_r} - r_r \omega_s i_{qs} \frac{L_m^2}{L_r^2} - \omega_s v_{qr} \frac{L_m}{L_r} \tag{13}$$

$$pe'_{qs} = -s\omega_s e'_{ds} - \frac{r_r e'_{qs}}{L_r} + r_r \omega_s i_{ds} \frac{L_m^2}{L_r^2} + \omega_s v_{dr} \frac{L_m}{L_r} \tag{14}$$

By substituting (5), (6), (11), and (12) into (1) and (2), we get:

$$\frac{L_m^2 - L_s L_r}{L_r} pi_{ds} = -v_{ds} + r_s i_{ds} - \frac{r_r e'_{qs}}{L_r \omega_s} - (\omega_r - \omega_s) e'_{ds} / \omega_s \cdots$$
$$\cdots + r_r \omega_s^2 i_{ds} \frac{L_m^2}{L_r^2} + \omega_s^2 v_{dr} L_m / L_r - L_s \omega_s i_{qs} - L_m \omega_s i_{qr} \tag{15}$$

$$\frac{L_m^2 - L_s L_r}{L_r} pi_{qs} = -v_{qs} + r_s i_{qs} + \frac{r_r e'_{ds}}{L_r \omega_s} - (\omega_r - \omega_s) e'_{qs} / \omega_s \cdots$$
$$\cdots + r_r i_{qs} \frac{L_m^2}{L_r^2} + v_{qr} L_m / L_r + L_s \omega_s i_{ds} + L_m \omega_s i_{dr} \tag{16}$$

Equations (13), (14), (15), and (16) will be used later in small signal stability analysis of Section III.

### B. Rotor Side/Grid Side Converter Controller Model

The converter model of DFIG consists of two pulse-width modulation invertors connected back to back via a capacitor. The objectives of GSC and RSC are to keep the capacitor voltage and to manage the real/reactive power of the stator-side in [11], respectively. The RSC/GSC control block diagram is shown in Fig. 2 and the equations are given by:

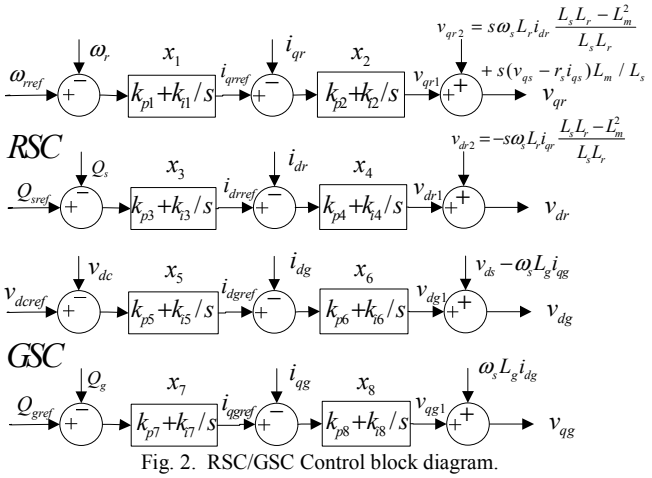


Fig. 2. RSC/GSC Control block diagram.

$$px_1 = \omega_{rref} - \omega_r \tag{17}$$

$$i_{qrref} = k_{p1}(\omega_{rref} - \omega_r) + k_{i1} x_1 \tag{18}$$

$$px_2 = i_{qrref} - i_{qr} = k_{p1}(\omega_{rref} - \omega_r) + k_{i1} x_1 - i_{qr} \tag{19}$$

$$v_{qr} = v_{qr1} + v_{q2} = k_{p2} k_{p1}(\omega_{rref} - \omega_r) + k_{p2} k_{i1} x_1 - k_{p2} i_{qr} + k_{i2} x_2 \cdots$$
$$\cdots s\omega_s L_r i_{dr} (L_s L_r - L_m^2) / (L_s L_r) + s(v_{qs} - r_s i_{qs}) L_m / L_s \tag{20}$$

$$px_3 = Q_{sref} - Q_s \tag{21}$$

$$i_{drref} = k_{p3}(Q_{sref} - Q_s) + k_{i3}x_3 \tag{22}$$

$$px_4 = i_{drref} - i_{dr} = k_{p3}(Q_{sref} - Q_s) + k_{i3}x_3 - i_{dr} \tag{23}$$

$$v_{dr} = v_{dr1} + v_{dr2} = k_{p4}k_{p3}(Q_{sref} - Q_s) + k_{p4}k_{i3}x_3 - k_{p4}i_{dr} \cdots + \cdots + k_{i4}x_4 - s\omega_s L_r i_{qr}(L_s L_r - L_m^2)/(L_s L_r) \tag{24}$$

$$px_5 = v_{dcref} - v_{dc} \tag{25}$$

$$i_{dgref} = k_{p5}(v_{dcref} - v_{dc}) + k_{i5}x_5 \tag{26}$$

$$px_6 = i_{dgref} - i_{dg} = k_{p5}(v_{dcref} - v_{dc}) + k_{i5}x_5 - i_{dg} \tag{27}$$

$$v_{dg} = v_{dg1} + v_{ds} - \omega_s L_g i_{qg} = k_{p6}k_{p5}(v_{dcref} - v_{dc}) + k_{p6}k_{i5}x_5 \cdots + \cdots - k_{p6}i_{dg} + k_{i6}x_6 + v_{ds} - \omega_s L_g i_{qg} \tag{28}$$

$$px_7 = Q_{gref} - Q_g \tag{29}$$

$$i_{qgref} = k_{p7}(Q_{gref} - Q_g) + k_{i7}x_7 \tag{30}$$

$$px_8 = i_{qgref} - i_{qg} = k_{p7}(Q_{gref} - Q_g) + k_{i7}x_7 - i_{qg} \tag{31}$$

$$v_{qg} = v_{qg1} + \omega_s L_g i_{dg} = k_{p8}k_{p7}(Q_{gref} - Q_g) + k_{p8}k_{i7}x_7 \cdots + \cdots - k_{p8}i_{qg} + k_{i8}x_8 + \omega_s L_g i_{dg} \tag{32}$$

The RSC and GSC are connected by a large capacitor (C) to decouple. The parameter $\omega_{rref}$ is the reference of the rotor speed which is determined by WT power speed characteristic for maximum power extraction [11]. Parameters $Q_{sref}, Q_{gref}, v_{dcref}$ are the references of reactive power of the stator/GSC, and capacitor voltage, and are set to zero, zero, and 4KV, respectively. Parameters $k_{pi}, k_{ii}, x_i \ (i = 1, \cdots 8)$, $v_{dg}, v_{qg}, i_{dg}, i_{dg}, L_g, s$ are the proportional gains/ the integrating gains of PI controllers, the state variables, the d/q axis voltage/current/ inductance of GSC winding, and the slip, respectively. By neglecting losses and harmonics, the power balance equation (between real power of RSC and real power of GSC) is given by:

$$P_r - P_g = Cv_{dc}Pv_{dc} \approx Cv_{dcref}Pv_{dc} \tag{33}$$

C. WT Model

The aerodynamic model of the WT can be described by the $C_{P-\lambda-\beta}$ curves [11]. Neglecting the pitch angle change and setting the power coefficient to the maximum value according to the unique wind speed, the mechanical power of WT extracted from the wind is given by:

$$P_m = 0.5\rho A_r v_w^3 C_p(\lambda) \tag{34}$$

where $\rho, A_r, v_w, \lambda$ are the air density, the area swept by the turbine blades, wind speed, and tip-speed-ratio, respectively. The shaft system of WT could be characterized by a two-mass system [11] and if the damping coefficients of the turbine and generator are set to zero, the electromechanical equations are given by:

$$2H_t p\omega_t = T_m - D_{tg}(\omega_t - \omega_r) - T_{tg} \tag{35}$$

$$2H_g p\omega_r = T_{tg} + D_{tg}(\omega_t - \omega_r) - T_e \tag{36}$$

$$pT_{tg} = K_{tg}(\omega_t - \omega_r) \tag{37}$$

$$T_m = P_m / \omega_t \ and \ T_e = L_m(i_{qs}i_{dr} - i_{ds}i_{qr}) \ in \ per-unit \tag{38}$$

where $T_m, T_e, T_{tg}, \omega_t, H_t, H_g, D_{tg}, K_{tg}$ are the mechanical torque, the electrical torque, the internal torque, the turbine rotor speed, the inertia constants of the turbine and the generator, the damping coefficient of the shaft between two masses, and the shaft stiffness, respectively. The $T_m, T_e$ can be eliminated by substituting (34) and (38) into (35) and (36).

D. Connected Points Model

Neglecting losses and applying the d/q frame transformation to the point which DFIG connects the grid and the GSC connects the stator winding, the voltage equations are given by [12]:

$$\begin{bmatrix} v_{ds} \\ v_{qs} \end{bmatrix} = \begin{bmatrix} \cos\theta \\ -\sin\theta \end{bmatrix} v_{grid} - \begin{bmatrix} 0 & -x_{TL} \\ x_{TL} & 0 \end{bmatrix} \begin{bmatrix} i_{ds} + i_{dg} \\ i_{qs} + i_{dg} \end{bmatrix} \tag{39}$$

$$\begin{bmatrix} v_{ds} \\ v_{qs} \end{bmatrix} = \begin{bmatrix} v_{dg} \\ v_{qg} \end{bmatrix} + \begin{bmatrix} 0 & -x_{tg} \\ x_{tg} & 0 \end{bmatrix} \begin{bmatrix} i_{dg} \\ i_{qg} \end{bmatrix} \tag{40}$$

where $v_{grid}, \theta, x_{TL}, x_{tg}$ are the grid voltage, the angle of the terminal voltage of DFIG stator winding, the combined reactance of the transformer and transmission line between DFIG and the grid, and the combined reactance of the transformer and GSC winding between GSC and the stator winding, respectively. More details can be found in the references [11], [12], and [15].

## III. SMALL SIGNAL STABILITY ANALYSIS

The SMIB-DFIG system could be represented by the set of differential and algebraic equations as:

$$\begin{cases} \dot{\mathbf{x}} = \mathbf{f(x, y)} \\ \mathbf{0} = \mathbf{g(x, y)} \end{cases} \tag{41}$$

where the 16 differential equations include (13) – (17), (19), (21), (23), (25), (27), (29), (31), (33), (35), (36), (37) and the 10 algebraic equations include (11), (12), (20), (24), (28), (32), (39), (40). Variables $P_r, P_g, Q_s, Q_g, T_m, T_e, \omega_{rref}, Q_{sref}, v_{dcref}$ are dependent variables, and are easily replaced by the state and other variables, and the initial values/set points.

The vector of 16 state variables:

$\mathbf{x}=[e'_{ds}, e'_{qs}, i_{ds}, i_{qs}, x_1, x_2, x_3, x_4, x_5, x_6, x_7, x_8, v_{dc}, \omega_t, \omega_r, T_{tg}]$.

The vector of 10 other variables:

$\mathbf{y}=[v_{ds}, v_{qs}, v_{dr}, v_{qr}, v_{dg}, v_{qg}, i_{dr}, i_{qr}, i_{dg}, i_{qg}]$.

Linearization of equation (41) at an operating point $(x_0, y_0)$ which is obtained by the load flow calculation, we can get:

$$\begin{bmatrix} \Delta\dot{\mathbf{x}} \\ 0 \end{bmatrix} = \begin{bmatrix} \mathbf{A\ B} \\ \mathbf{C\ D} \end{bmatrix} \begin{bmatrix} \Delta\mathbf{x} \\ \Delta\mathbf{y} \end{bmatrix} \tag{42}$$

The **A, B, C, D** are the partial derivatives of functions **f(x, y)** and **g(x, y)** with respect to the variables **x** and **y,** respectively**.** The system matrix can be calculated as:

$$\Delta\dot{\mathbf{x}} = \mathbf{A_{sys}}\Delta\mathbf{x} \ and \ \mathbf{A_{sys}} = \mathbf{A - BD^{-1}C} \tag{43}$$

The eigenvalues $\lambda_i$ ($\lambda_i = \sigma_i + j\omega_i$, $i = 1, \cdots 16$) of state matrix are easily obtained and the damping ratios and frequencies of $\lambda_i$

are given by: $\zeta_i = \left| \sigma_i / \sqrt{(\sigma_i^2 + \omega_i^2)} \right|$ *and* $f_i = \left| \omega_i / 2\pi \right|$ (44)

When the damping ratios are large enough, the system can quickly go to the initial steady state because the oscillations are well damped and the small signal stability is significantly improved. Therefore, an optimization problem can be formulated to maximize the damping ratios. Since the low frequency oscillations are serious cause for concerns in DFIG system, the optimization is simply adjusted and given by:

Objective function: $F = \max\ \zeta_i,\ \textit{where}\ f_i \subset [0.5,\ 1.5]$ (45)

Control variables: $K_i$ and $K_p$ of DFIG PI controllers.

Constraints: $K_i$ and $K_p$ are in the range $[K_{imin},\ K_{imax}]$ and $[K_{pmin},\ K_{pmax}]$, respectively.

This will ensure that the low frequency oscillations (frequency in 0.5~1.5Hz) are well damped in small signal stability analysis.

## IV. PSO AND ANN TRAINING

Particle swarm optimization (PSO) is an evolutionary computation technique and inspired by the paradigm of birds flocking [16]. It starts from a group of initial positions (particles) in the space so as to increase the possibility to find the optimal position. Compared with other evolutionary algorithms, such as genetic algorithms (GAs), Tabu search algorithms, and simulated annealing algorithms, PSO possesses many attractive properties such as memory and constructive cooperation, so it has more chances to find the better solution and discover reasonable quality solution much faster. Moreover, PSO isn't easy to degrade when the parameters being optimized are highly correlated [11]. Usually, the searching procedure of PSO includes 4 steps: initialization, evaluation, stopping criterion, and updating velocities and positions.

Artificial neural network (ANN) consists of highly interconnected simple processing units designed in a way to model how human brain performs a particular task [17]. It is essentially a mathematical model of a non-linear statistical data modeling tool and is a powerful and simple algorithm to approximate nonlinear functions or to solve problems where the input-output relationship is neither well defined nor easily computable. Generally, the procedure of ANN includes 3 steps: model selection, training and learning algorithm, and evaluation.

In this paper, the historical data set (including 50 input data set-wind speed and 50 output data set-optimal PI parameters calculated by PSO) is used to train a two-layer feed-forward ANN in which the first layer has one input (wind speed) and ten TANSIG neurons and the second layer has one PURELIN neuron (TANSIG and PURELIN are transfer functions of ANN in common use) [18]. The mathematical function of the ANN is given by:

$$k = \left[ \sum_{i=1}^{10} \left[ \left( \frac{2}{\left(1 + e^{(-2(IW_i * v_w + B1_i))}\right)} - 1 \right) * LW_i \right] \right] + BL \quad (46)$$

After sufficient historical data training, ANN construction parameters ($IW_i$, $B1_i$, $LW_i$, and BL) [19] can be obtained so that ANN can quickly forecast the optimal PI parameters at any wind speed now. Therefore, the ANN optimal DFIG model can maintain optimal transient performance in all wind speeds range via ANN controllers to dynamically adjust PI controller parameters. The ANN control block diagram is shown in Fig. 3 and the overall design flowchart is shown in Fig. 4:

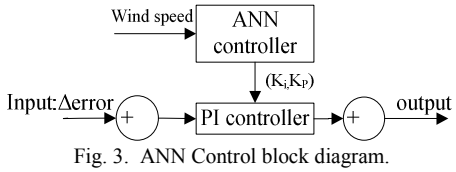


Fig. 3. ANN Control block diagram.

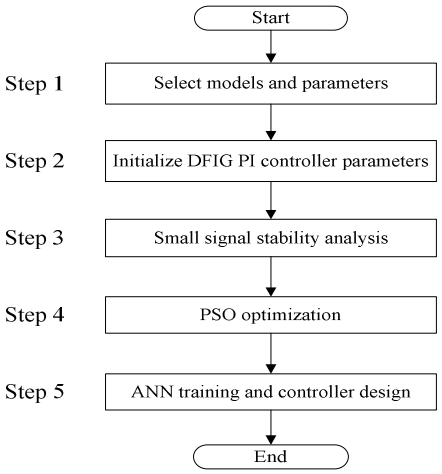


Fig. 4. Flowchart of ANN optimal DFIG model design procedure.

## V. SIMULATION RESULTS

The SMIB shown in Fig.1. is simulated via PSCAD software to prove the transient performance improvement by comparing three models: the initial DFIG model, the fix-optimal DFIG model (only optimizing PI parameters at wind speed=11m/s based on small signal stability analysis), and the ANN optimal DFIG model. The main differences among three models are the PI controller parameters. The disturbances are given as follows:

*1)* At t=0 second, the wind speed is 11m/s and GSC/RSC controllers are not working at first.

*2)* At t=0.001 second, GSC and RSC start. The purpose of this simulation is to prove the cut-in impact of DFIG.

*3)* At t=4 second, the three-phase short circuit happens in transmission line near the infinite bus and clears at t=4.7 second. In this fault, the voltage of DFIG connected to the grid decreases to 0.5p.u. in order to investigate the low voltage ride-through capability of DFIG.

*4)* At t=10 second, the wind speed has a step change from 11m/s to 13m/s and this is to check the wind step change impact of DFIG.

The results of the three models' rotor speed, real power, mechanical torque, connection point voltage, DC-link capacitor voltage, and rotor q axis current, are shown in Figures 5-10, respectively. Comparing the results between the ANN optimal model and the initial model, it can be verified that the advantages of the ANN optimal model are numerous during the disturbances of cut-in, short circuit fault, wind speed step change, especially considering $T_m$, $P_o$, $I_{qr}$, and $v_{dc}$. The low frequency oscillations are greatly reduced. The

indices, such as eigenvalues, damping ratios, peak values, dynamic impacts, and settling times, as well as stability of the ANN optimal model are improved significantly compared to the initial model. The peak value reductions are very useful to reduce WT stochastic output and the impacts to the grid. The oscillation of $T_m$ is well damped to improve the performance of WT's gearbox which is the most easily damaged equipment. The oscillations of $v_{dc}$, $I_{qr}$ are reduced significantly, thus contributing to better DFIG safety. The connection point voltage of the ANN optimal model recovers to 0.995p.u. two second faster than the initial model and it is very imperative to the grid voltage stability.

Comparing the results between the fix-optimal model and the ANN optimal model, they almost have the same transient performances for the cut-in and short circuit fault disturbances. However, for the wind speed step change disturbance which is the most common disturbance, the peak/trough values of $w_r$, $P_o$, $T_m$, and $I_{qr}$ of two models are varied from 1.181 to 1.109 p.u., from -3.2 to -2.10 MW, from 0.57 to 0.25 p.u., and from -0.67 to -0.38 p.u., respectively. This makes the ANN optimal model holds an obvious advantage when the wind speeds change frequently and rapidly. This is particularly important since this disturbance may occur hundreds of times in one day, and therefore improving the transient performance subject to speed changes is crucial. This is the most important contribution of the paper.

Although the value of $v_{dc}$ peak of the ANN optimal model is 4.80KV during the cut-in disturbance, this value is still in an appropriate range, especially comparing it to the trough of the initial model which $v_{dc}$ decreases to 2.75KV. The reason may be that the ANN controllers are highly sensitive. However, this is not a noticeable drawback of the ANN optimal model.

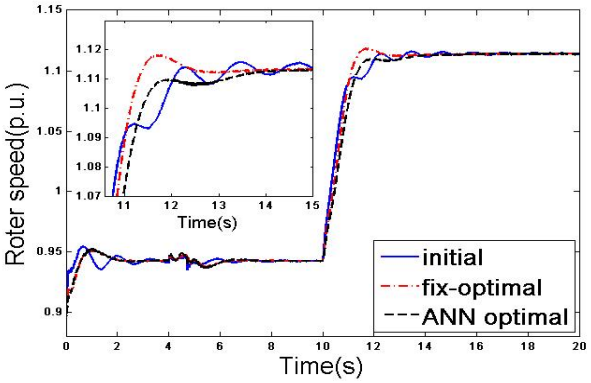

Fig. 5. Simulation results of rotor speed $w_r$

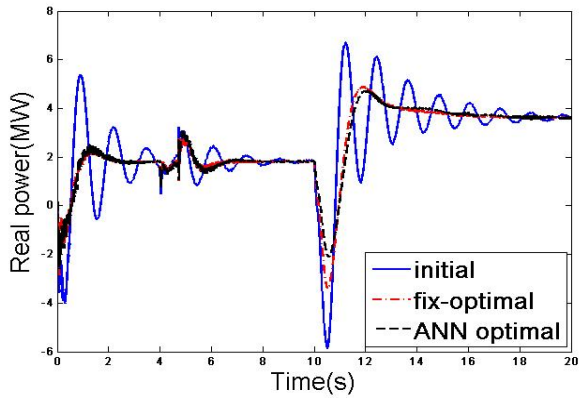

Fig. 6. Simulation results of real power $P_o$

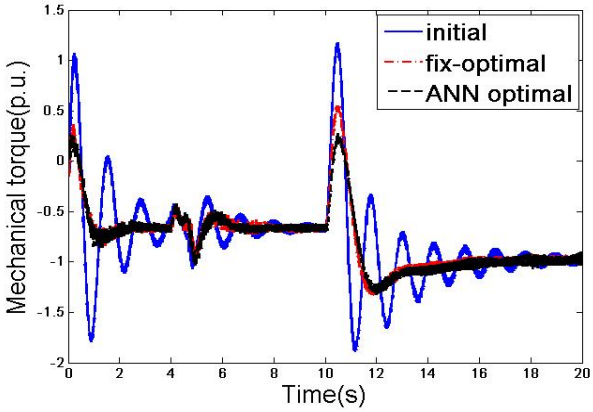

Fig.7. Simulation results of mechanical torque $T_m$

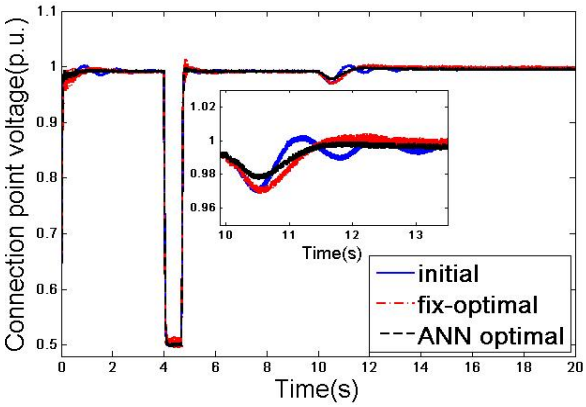

Fig.8. Simulation results of connection point voltage $v_s$

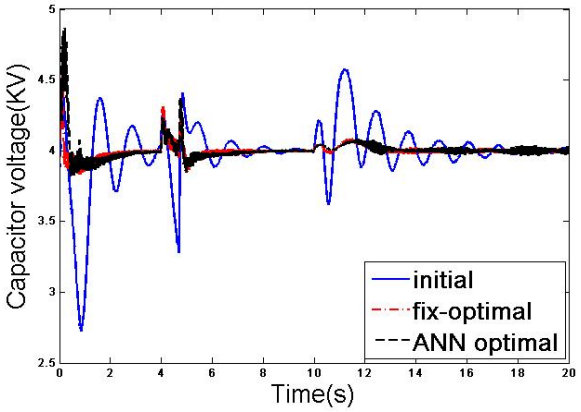

Fig. 9. Simulation results of DC-link capacitor voltage $v_{dc}$

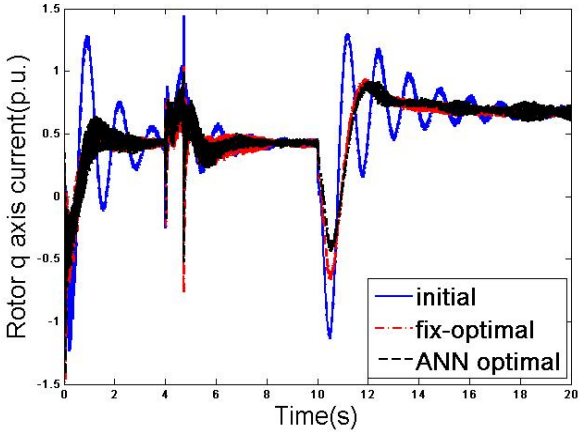

Fig.10. Simulation results of rotor q axis current $I_{qr}$

## VI. Conclusion

A novel artificial neural network (ANN)-based adaptive PI control doubly fed induction generator (DFIG) driven by a wind turbine has been designed and connected to the power grid. Particle swarm optimization (PSO) algorithm is used to determine the optimal parameters of DFIG PI controllers at different operating points in small signal stability analysis. An ANN which has a simple structure and a sufficient accuracy is designed, trained, and it provides the ability to quickly forecast the optimal parameters. The ANN controllers dynamically change PI gain values according to the different wind speed to increase DFIG transient performance in a global operating range. The simulation results show that the proposed algorithm is highly efficient to reduce DFIG low frequency oscillations. The indices of eigenvalues, damping ratios, etc, verify that the transient performance of DFIG is significantly improved in a wide wind speed range while the stability is also improved.

## VII. Acknowledgment

The authors are grateful to the Nebraska Center for Energy Sciences Research for their support of this project.

## VIII. Appendices

Appendix A: Parameters of the SMIB system (60Hz, p.u.)

TW rated capacity: 3.6MW, number of blades: 3, rotor diameter: 104 m, swept area: 8495 $m^2$, $H_t$= 4.29s, $H_g$= 0.9s, $D_{tg}$ =1.5, $K_{tg}$ =296.7.

DFIG (4.16kV, 3.6MW): $r_s$= 0.0079, $r_r$= 0.025, $L_{ls}$= 0.07937, $L_{lr}$= 0.40, $L_m$= 4.4, $L_g$=0.005, $x_{tg}$= 0.05, C= 0.02F.

Power grid (34.5 kV): $r_{l1} = r_{l2}$ =0.014, $x_{l1} = x_{l2}$ =0.08, $x_{TL}$ =0.051,

Appendix B: Parameters of PSO algorithm

N=25, n=100, w=0.9, c1=c2=2.

Lower and upper bounds of PI controllers Bound:

$[K_{p1},K_{p2},K_{p3},K_{p4},K_{p5},K_{p6},K_{p7},K_{p8},K_{i1},K_{i2}, K_{i3}, K_{i4},K_{i5},K_{i6},K_{i7},K_{i8}]$;

LB=[0.02,0.1,0.1,0.1,0.1,0.1,0.002,0.1,0.05,0.1,5,5,0.2,50,5,50];

UB=[1,5,5,5,3,5,0.5,5,1,50,150,150,5,300,100,310].

Appendix C: Parameters of the initial DFIG model

$K_{p1}$=0.2, $K_{p2}$=0.7, $K_{p3}$=1.0, $K_{p4}$=2.0, $K_{p5}$=0.5, $K_{p6}$=1.5, $K_{p7}$=0.05, $K_{p8}$=1.5;

$K_{i1}$=1, $K_{i2}$=0.333, $K_{i3}$=10.0, $K_{i4}$=25.0, $K_{i5}$=1.0, $K_{i6}$=161.29, $K_{i7}$=20.0, $K_{i8}$=161.29.

Appendix D: Parameters of the fix-optimal DFIG model at wind (11m/s)

$K_{p1}$=0.08, $K_{p2}$=5.0, $K_{p3}$=4.0, $K_{p4}$=5.0, $K_{p5}$=3.0, $K_{p6}$=4.92, $K_{p7}$=0.2, $K_{p8}$=4.5;

$K_{i1}$=0.13, $K_{i2}$=2.0, $K_{i3}$=149.25, $K_{i4}$=50.0, $K_{i5}$=4.88, $K_{i6}$=222.22, $K_{i7}$=98.04, $K_{i8}$=303.03.

## IX. References


[1] "Global wind energy outlook 2008", Global Wind Energy Council, Oct. 2008 (available online: http://www.gwec.net/index.php?id=92).

[2] Muller S., Deicke M. "Doubly fed induction generator systems for wind turbines," IEEE industry application magazine, May /June 2002.

[3] P. B. Erikson, T. Ackermann, H. Abildgaard, P. Smith, W. Winter, and J. M. Rodriguez Garcia, "System operation with high wind penetration," IEEE Power Energy magazine, Vol. 3, No. 6, pp. 65-74, Nov 2005

[4] Wei Qiao, Harley R.G, "Effect of grid-connected DFIG wind turbines on power system transient stability," Power and Energy Society General Meeting - Conversion and Delivery of Electrical Energy in the 21st Century, pp. 1-7, 20-24 July 2008.

[5] F. M. Hughes, Olimpo Anaya-Lara, "A Power System Stabilizer for DFIG-Based Wind Generation," Power Systems, IEEE Transactions on Volume 21, Issue 2, pp. 763-772, May 2006.

[6] F. Mei and B. C. Pal, "Modeling analysis of grid connected doubly fed induction generator", IEEE Transactions on Energy Convers., Volume 22, No. 3, pp. 728-736, Sep 2007.

[7] Mustafa Kayikçi, J.V.Milanovic, "Assessing Transient Response of DFIG-Based Wind Plants—the Influence of Model Simplifications and Parameters," IEEE Transactions on power systems, Vol. 23, No. 2, pp. 545-554, May 2008

[8] Singh B., Emmoji V., Singh S.N., "Performance evaluation of series and parallel connected grid side converters of DFIG," Power and Energy Society General Meeting - Conversion and Delivery of Electrical Energy in the 21st Century, 2008 IEEE, pp. 1-8, 20-24 July 2008.

[9] F.M. Hughes, Olimpo Anaya-Lara, "A Power System Stabilizer for DFIG-Based Wind Generation," Power Systems, IEEE Transactions on Volume 21, Issue 2, pp. 763-772, May 2006.

[10] Muyeen, S. M, Takahashi, R, Murata, T, Tamura, J, "Integration of an Energy Capacitor System with a Variable-Speed Wind Generator," Power Systems, IEEE Transactions on Volume 25, Issue 1, pp. 331-340, Feb 2010.

[11] Wei Qiao, G. K. Venayagamoorthy, and R. G. Harley, "Design of optimal PI controllers for doubly fed induction generators driven by wind turbines using particle swarm optimization," in 2006 International Joint Conference on Neural Networks, Canada, pp. 1982-1987, Jul 2006

[12] F. Wu, X. P. Zhang, K. Godfrey, "Small Signal Stability Analysis and Optimal Control of a Wind Turbine with Doubly Fed Induction Generator," IET Generation, Transmission & Distribution , Volume 1, Issue 5, pp. 751-760, 2007.

[13] Y. Mishra, S. Mishra, Fangxing Li, Z. Y. Dong, "Small Signal Stability Analysis of a DFIG Based Wind Power System with Tuned Damping Controller under Super/Sub-Synchronous Mode of Operation," 2009 PES General Meeting, 26-30 JULY 2009.

[14] D. W. Novotny and T. A. Lipo, "Vector Control and Dynamics of AC Drive," Oxford University Press, 2000.

[15] Kundur, P., "Power System Stability and Control," Mcgram-Hill, Inc, New York,1994, pp. 279-306

[16] Kennedy, J., and Eberhart, R., "Particle swarm optimization," Proc. IEEE Int. Conf. on Neural Network, Perth, Australia, vol. IV, pp. 1942-1948, 1995,

[17] S. Haykin, "Neural Networks: A Comprehensive Foundation," New Jersey: Prentice-Hall, 1999

[18] Vogl, T. P., J.K. Mangis, A.K. Rigler, W.T. Zink, and D.L. Alkon, "Accelerating the convergence of the back propagation method," Biological Cybernetics, vol. 59, pp. 257-263, 1988.

[19] S. N. Sivanandam, Sumathi & Deepa, "Introduction to neural networks using MATLAB 6.0," Tata McGraw-Hill Education, 2006